

X-Ray Diffraction, FTIR, and NMR Characterization of Sol–Gel Alumina Doped with Lanthanum and Cerium

A. Vázquez,^{*} T. López,^{*,†} R. Gómez,^{*,†} Bokhimi,^{‡,§,1} A. Morales,[‡] and O. Novaro^{‡,2}

^{*}Department of Chemistry, Universidad Autónoma Metropolitana-Iztapalapa, A.P. 55-534, 09340 México, D.F., Mexico; [†]Universidad de Guanajuato, Lascruain de Retana s/n, Guanajuato, Gto., Mexico; [‡]Institute of Physics, National University of Mexico (UNAM) A.P. 20-364, 01000 México, D.F., Mexico; and [§]National Institute of Nuclear Research (ININ), México, D.F., Mexico

Received December 13, 1995; in revised form August 27, 1996; accepted August 28, 1996

Alumina doped with La and Ce was prepared by using the sol–gel technique. The doping concentrations were alternatively 2 and 5 wt% for each element. Samples were characterized as a function of temperature by using X-ray powder diffraction and FTIR spectroscopy. MAS-NMR studies showed that lanthanum and cerium interacted with alumina and produced a compound with aluminum ions in tetrahedral symmetry. These interactions stabilized alumina structure and shifted its transformations to higher temperatures. When cerium-doped samples were heated at temperatures higher than 1000 °C, CeO₂ was segregated. For La doping such segregation was not observed. Brønsted acid sites were generated for the low doping concentrations of both elements. At the high doping concentration, however, only Lewis acid sites existed in a higher concentration than in undoped alumina. © 1997 Academic Press

1. INTRODUCTION

In the traditional synthesis of alumina, the initial precursor hydroxide determines its different phases and properties (1–6).

Alumina of high thermal stability and high specific surface area is obtained by using the sol–gel technique (7–10). Usually, Al and O atoms form a nearly amorphous structure, with Al³⁺ and O²⁻ ions forming octahedra (11).

When supercritical drying is used in the sol–gel process, aerogel alumina is obtained (12,13). This alumina has a large specific surface area and macropores that make it attractive for use as a support in catalysis, because it favors the interaction with the metal to be supported.

The sol–gel process also can produce xerogel alumina (14–19). Xerogels are made from a colloidal solution gelling at low temperatures at atmospheric pressure. They are solids with collapsed porosity produced by the surface stress

generated during dehydration and dehydroxylation. Preparation, aging, and drying procedures determine the final xerogel properties (19, 20).

When γ -alumina is doped with La and Ce it is stabilized and used as a support in catalysis (21–26). CeO₂ and La₂O₃ not only stabilize γ -alumina but also improve its selectivity to definite products. Cerium is the most frequent base additive used in the support of automobile converter catalysts that transform carbon monoxide, hydrocarbons, and nitrogen oxides (27–29). Cerium-doped catalysts can supply oxygen in reduction and oxidation environments. The stabilization of γ -alumina by La is supposed to be caused by nucleation of LaAlO₃ on the alumina surface (21). LaAlO₃ interacts with the γ -alumina support and inhibits its transformation toward α -alumina.

In this work, we synthesized alumina xerogels doped with La and Ce. These xerogels were characterized by X-ray powder diffraction and FTIR spectroscopy after being heated at different temperatures. They were also characterized by MAS-NMR spectroscopy.

2. EXPERIMENTAL

Synthesis of sol–gel Al₂O₃. Aluminium *sec.*-butoxide, Al(OC₄H₉s)₃ (0.207 mol) was mixed with 6.5 mol of absolute ethanol at 60°C, refluxing and stirring constantly. Distilled water (2.94 mol) was added to this mixture, giving a water/alkoxide molar ratio of 14.2. The gelling reaction was completed 1 h after having added this solution. Thereafter, the gel was dried in air at 70°C for 24 h.

Synthesis of sol–gel La/Al₂O₃ with 2 and 5 wt% La. Aluminium *sec.*-butoxide (0.207 mol) was mixed with 6.5 mol of absolute ethanol at 60°C, refluxing and stirring constantly. For each La concentration, a water solution of lanthanum nitrate containing 2.94 mol of distilled water was added to this mixture. The gelling reaction was completed 1 h after having added this solution. Thereafter, the gels were dried under the same conditions as alumina gel. After drying at

¹ To whom correspondence should be addressed.

² Member of El Colegio Nacional, Mexico.

70°C, the samples of all three systems were annealed in air for 12 h at temperatures between 500 and 1100°C.

Synthesis of sol-gel Ce/Al₂O₃ with 2 and 5 wt% Ce. Aluminium *sec.*-butoxide (0.207 mol) was refluxed with 6.5 mol of absolute ethanol at 60°C, stirring constantly. For each Ce concentration, a water solution of cerium nitrate containing 2.94 mol of distilled water was added. The gelling reaction was completed 1 h after having added this solution. Thereafter, the gels were dried under the same conditions as alumina gel.

X-ray powder diffraction. The structure (crystalline or amorphous) of the phases in the samples, annealed at different temperatures, was obtained at room temperature by using X-ray powder diffraction. The reflection diffractometer used CuK α radiation, and had a graphite monochromator in the secondary beam. Each specimen was prepared by packing sample powder in a glass holder. Intensity data were measured by step scanning in the 2θ ranges between 2° and 110° and between 2° and 70°, with a 2θ step of 0.02° and a measuring time of 1 s per point.

FTIR spectroscopy. The dried solids were characterized *in situ* with a Nicolet 170-SX Fourier spectrometer, which uses controlled atmospheres. Before measuring, samples were pressed until transparency was achieved. Spectra were measured in a vacuum of 1×10^{-6} Torr. To identify and characterize the acid sites, pyridine was adsorbed by fluxing N₂ on the samples at room temperature. Pyridine excess was removed by making a vacuum in the camera of the spectrometer. During the analysis *in situ*, pyridine was desorbing while the samples were heated to 300°C.

MAS-NMR spectroscopy. Powder of the samples was analyzed in a Bruker NMR spectrometer Model ASX-300. The study was done with the ²⁷Al isotope at a frequency of 78.21 MHz with a spinning speed of 12 kHz. Chemical shifts were referred to aluminum in Al(H₂O)₆³⁺ ion.

3. RESULTS AND DISCUSSION

X-ray Diffraction Analysis

The X-ray diffraction patterns of the fresh dried samples in all systems were similar (Figs. 1–5). They corresponded to an aluminum hydroxide with a crystalline structure having some diffraction peaks as in bohemite (5) and others diffraction peaks as in δ -Al(OH)₃ (30). The crystalline structure, however, did not correspond to any of them.

Undoped sol-gel alumina was transformed into γ - and α -alumina when it was annealed in air (Fig. 1). After the sample was heated at 1000°C, γ -alumina and impurities of α -alumina were formed. The transformation of amorphous into γ -alumina was associated with the dehydration of the sample hydrated during the sol-gel process. When the sample was heated from 1000 to 1100°C, the γ -alumina was

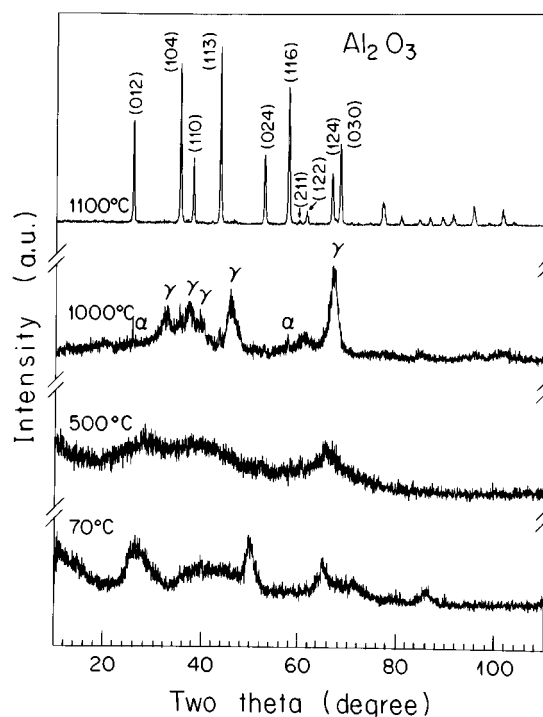


FIG. 1. X-ray powder diffraction pattern of undoped sol-gel alumina after annealing the sample at different temperatures. α and γ indicate α - and γ -alumina. The indexing of the pattern corresponds to α -alumina.

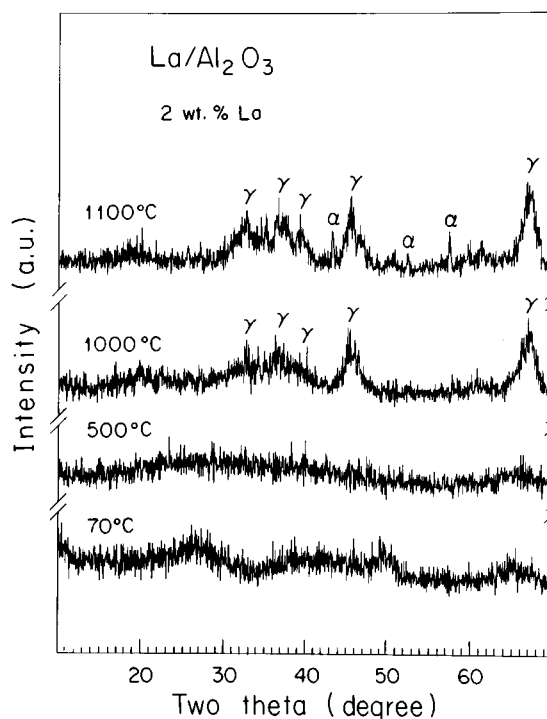


FIG. 2. X-ray powder diffraction pattern of sol-gel La/Al₂O₃ with 2 wt% La after annealing the sample at different temperatures. α and γ indicate α - and γ -alumina.

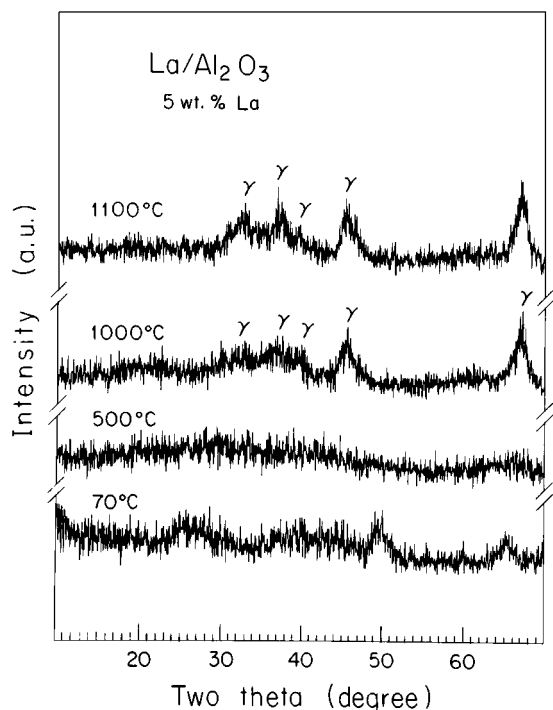


FIG. 3. X-ray powder diffraction pattern of sol-gel La/Al₂O₃ with 5 wt.% La after annealing the sample at different temperatures. γ indicates γ -alumina.

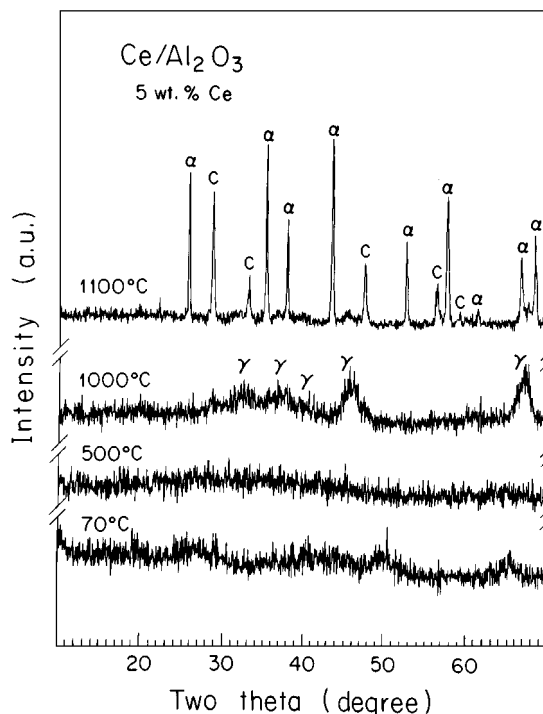


FIG. 5. X-ray powder diffraction pattern of sol-gel Ce/Al₂O₃ with 5 wt.% Ce after annealing the sample at different temperatures. α , γ , and c indicate α - and γ -alumina and cerianite, respectively.

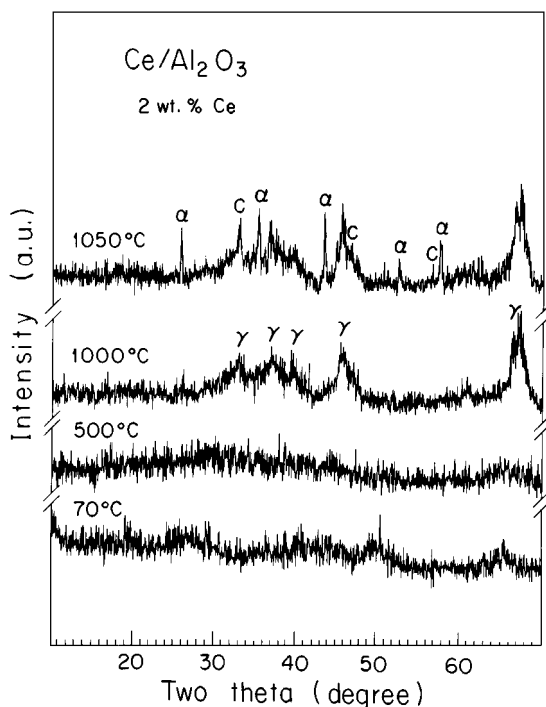


FIG. 4. X-ray powder diffraction pattern of sol-gel Ce/Al₂O₃ with 2 wt.% Ce after annealing the sample at different temperatures. α , γ , and c indicate α - and γ -alumina and cerianite, respectively.

totally transformed into α -alumina, which has a MAS-NMR spectrum with a chemical shift of -2.1 ppm (Fig. 6), which falls in the range of chemical shifts corresponding to aluminum ions with octahedral symmetry (31).

Lanthanum doping of sol-gel alumina inhibited the transformation of alumina phases (Figs. 2 and 3). After these doped samples were heated at 500°C in air, the structure was amorphous, but, after heating at 1000°C, it transformed into γ -alumina, which was stable even at 1100°C. The MAS-NMR spectrum of the sample heated at this temperature (Fig. 6) shows one peak at -3.6 ppm and a second peak that was very broad and centered around 35 ppm. The first peak corresponds to an aluminum ion in octahedral symmetry; the second one corresponds to an aluminum ion in tetrahedral symmetry (31). Since the area of the first peak is larger (Fig. 6), more aluminum ions are in octahedral symmetry. At this temperature, however, the X-ray diffractogram shows that almost all sample is γ -alumina. The number of sites with tetrahedral symmetry increases with La concentration (Fig. 6). The sample with 2 wt% La had impurities of α -alumina (Fig. 2), in contrast to the sample corresponding to 5 wt% La (Fig. 3). This means that for totally stabilizing the sample in the γ -alumina phase, the concentration of 2 wt% is insufficient.

The X-ray diffraction patterns of the La-doped samples, however, did not show the presence of the LaAlO₃ phase

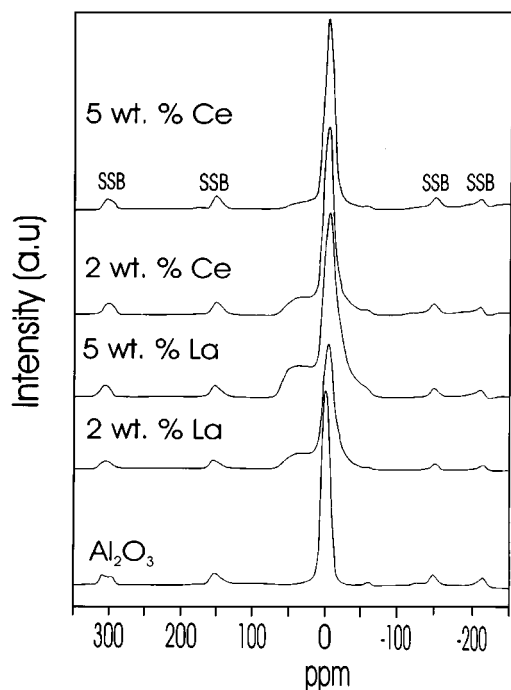


FIG. 6. MAS-NMR spectra of the samples after annealing them at 1100°C: (a) sol-gel Al_2O_3 , (b) 2 wt% $\text{La}/\text{Al}_2\text{O}_3$, (c) 5 wt% Al_2O_3 , (d) 2 wt% $\text{Ce}/\text{Al}_2\text{O}_3$, and (e) 5 wt% $\text{Ce}/\text{Al}_2\text{O}_3$. SSB in the figure indicates the spinning side bands.

reported to be responsible for the stability of La-doped alumina (21). In this phase aluminum ion has octahedral symmetry, and according to the MAS-NMR spectra, lanthanum doping gives rise to aluminum ions with tetrahedral symmetry. LaAlO_3 did not appear even after the sample was heated at 1200°C; at this temperature the only crystalline phase observed was α -alumina. This suggests that in the present case La atoms were integrated into the alumina structure instead of being supported on the surface (21).

Lanthanum doping stabilized γ -alumina. Lanthanum and aluminum ions interacted and produced a local arrangement with aluminum ions in tetrahedral symmetry. This eliminated LaAlO_3 as the phase responsible for the alumina's stability, because in this phase the aluminum ion has octahedral symmetry.

Cerium doping also inhibited the transformation of alumina phases (Figs. 4 and 5). After these samples were heated at 500°C in air, they had an amorphous structure that was transformed into γ -alumina after heating at 1000°C. Here, Ce stabilized this structure, at least to this temperature. By heating the sample at 1050°C (Fig. 4), doped γ -alumina was partially transformed into α -alumina and cerianite (CeO_2). MAS-NMR analysis after annealing the sample at this temperature (Fig. 6) showed that cerium doping gave rise to aluminum ions with tetrahedral sym-

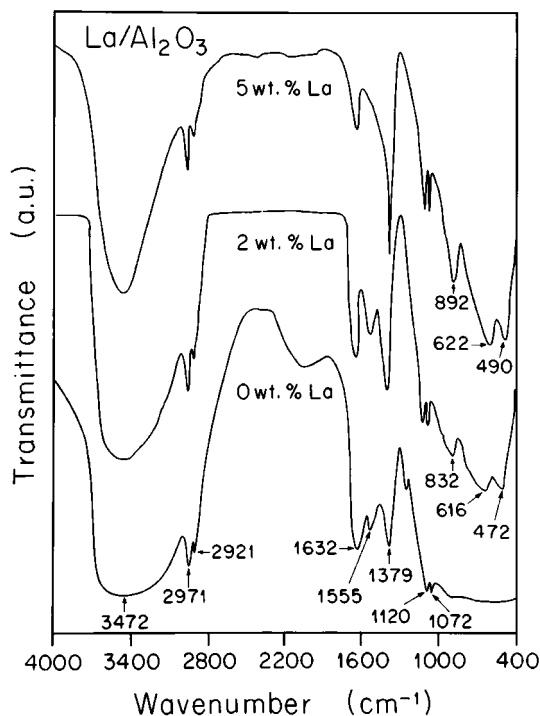


FIG. 7. FTIR spectra of the $\text{La}/\text{Al}_2\text{O}_3$ samples.

metry, similar to the way lanthanum did. The transformation of γ -alumina into α -alumina was nearly total at 1100°C (Fig. 5). This transformation also destroyed Al-Ce interaction, decreasing with that the number of aluminum ions with tetrahedral symmetry (Fig. 6). At this temperature, Ce, Al, and O did not combine to give a CeAlO_3 crystalline phase (32); instead, they segregated, forming Al_2O_3 and CeO_2 .

Ce doping also stabilized alumina phases. The stabilization was weaker than with La. Since the interaction between cerium and aluminum ions gave rise to aluminum ions with tetrahedral symmetry (Fig. 6), the CeAlO_3 phase was eliminated as being the phase responsible for the alumina's of stability. In CeAlO_3 aluminum ion has octahedral symmetry.

FTIR Studies

In the sol-gel alumina, the vibrations of OH ions and, C-H, Al-OH, and Al-O bonds generated the observed bands in the infrared region. The stretching vibration of the OH ions of residual water and solvent in the gel produced a very intense broadband at 3472 cm^{-1} (Fig. 7), whereas their bending vibration generated the band at 1632 cm^{-1} . The two small bands at 2971 and 2921 cm^{-1} were produced by the asymmetric bending vibrations of the C-H bond in the uncondensed butoxy groups. The stretching vibrations

of the Al–OH bond gave rise to the band at 1555 cm^{-1} . The weak bands observed at 1120 and 1072 cm^{-1} were produced by the Al–O bonds. The spectrum at low energies was undefined.

The high-energy infrared spectrum of La-doped alumina with 2 wt% La (Fig. 7) was similar to that observed for undoped alumina. The OH ions produced the same bands reported for these ions in undoped alumina. The intensity of the band at 2971 cm^{-1} produced by the asymmetric vibrations of the C–H bond, however, slightly decreased in intensity, but the band at 2921 cm^{-1} completely disappeared, indicating that the aluminum *sec.*-butoxide reaction was completed and that the amount of residual butoxy groups was low. The band at 1555 cm^{-1} observed in undoped alumina and produced by the vibrations of the Al–OH bond shifted to 1588 cm^{-1} and had a higher intensity. This shift was produced by the interaction of lanthanum ions with alumina.

Contrasting with undoped alumina FTIR spectrum, the low-energy region of the La-doped alumina spectrum was well defined. It showed bands at 832 , 616 , and 472 cm^{-1} , which probably were produced by vibrations of Al–O bonds corresponding to aluminum ions with tetrahedral symmetry.

Doping alumina with 5 wt% of La produced bigger changes (Fig. 7). For example, the band at 1555 cm^{-1} disappeared, indicating the absence of Al–OH bonds. The bands in the low-energy region moved to the higher energies, 892 , 622 , and 490 cm^{-1} . This shift was produced by a stronger Al–O bond corresponding to the higher stability of the structure than in undoped alumina.

The FTIR spectrum of Ce/Al₂O₃ with 2 wt% Ce was very similar to that of undoped alumina (Fig. 8). The principal differences were in the high-energy region. Here, Ce stabilized OH groups, causing the band produced by its stretching vibrations to move to 3352 cm^{-1} . For 2 wt% Ce the band at 1555 cm^{-1} , associated with Al–OH bonds, shifted to 1520 cm^{-1} , but it disappeared for 5 wt% Ce. As with undoped alumina, the spectrum at low energies was undefined. These results also suggest that the interaction between aluminum and cerium ions is weaker than that between aluminum and lanthanum ions.

Pyridine Adsorption Studies

When materials are produced by the sol–gel technique, the OH groups play an important role in the acidity of the product. For example, dehydration of alumina produces an acid–base site pair. In general, the most common acid sites are of the Lewis type, but in sol–gel alumina Brønsted sites are also generated.

The acidic properties and the nature of the sites generated in the samples are determined by studying the adsorption of pyridine as a function of temperature and its desorption in

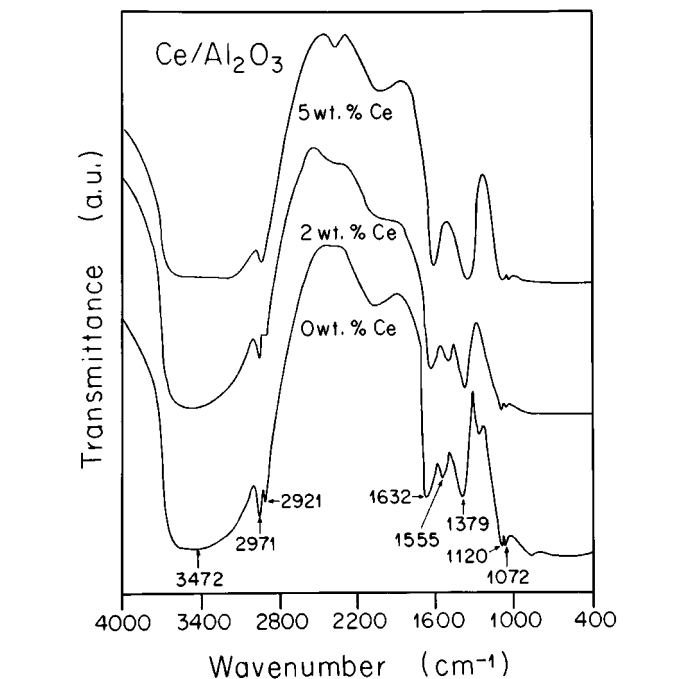


FIG. 8. FTIR spectra of the Ce/Al₂O₃ samples.

a vacuum (33). Pyridine is chemisorbed on oxides in two ways: on Lewis acid sites (coordinatively unsaturated or electron-pair acceptor sites) by coordination of nitrogen lone pair of electrons, and on Brønsted acid sites by transfer of protons from the site to nitrogen (34). With this method the Brønsted acid sites (protonic acidity) can be clearly distinguished from the Lewis acid sites (nonprotonic acidity), because Brønsted sites produce the pyridinium ion (PyH⁺) and promote the formation of pyridine species bonded to hydrogen, which produce the bands in the FTIR spectrum between 1700 and 1400 cm^{-1} .

In undoped alumina only Lewis acid sites were present. In these samples, the adsorption of pyridine produced two principal bands in the FTIR spectrum (Fig. 9), one at 1590 cm^{-1} and another at 1442 cm^{-1} , with a relative intensity of 2.1; they were characteristic of Lewis acid sites. Another band with a relative intensity of 0.4 appeared at 1490 cm^{-1} . The sample acidity was low and the acid sites disappeared with temperature; therefore, after the sample was heated at 300°C the intensity of the bands almost vanished.

The bending vibration of the OH ions of residual water and solvent in the gel gave rise to a band at 1632 cm^{-1} with an intensity decreasing with temperature (Fig. 9) because of sample dehydration.

Doping alumina with 2 wt% La generated Lewis and Brønsted acid sites. The acidity produced by Lewis acid sites gave rise to one band at 1448 cm^{-1} with a relative intensity

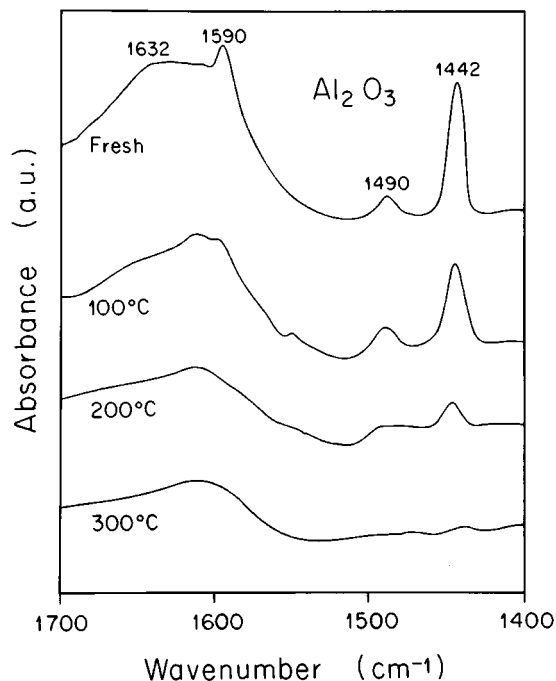


FIG. 9. FTIR spectra of pyridine adsorbed in sol-gel alumina.

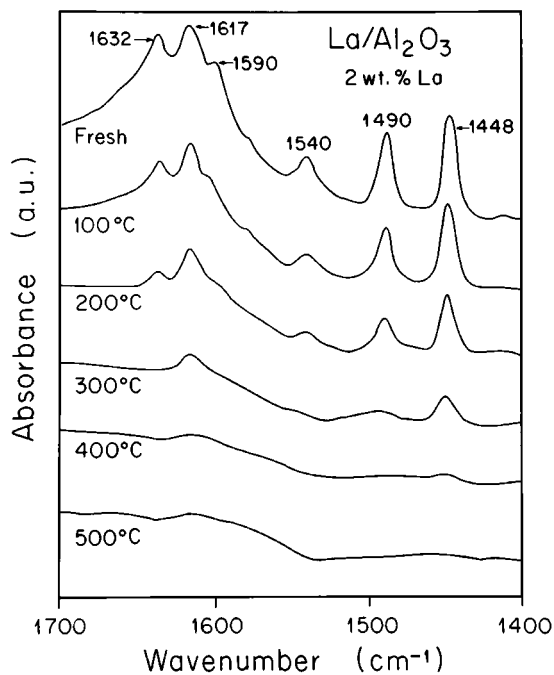


FIG. 10. FTIR spectra of pyridine adsorbed in a sol-gel $\text{La}/\text{Al}_2\text{O}_3$ sample with 2 wt% La.

of 2.56 and another at 1490 cm^{-1} with a relative intensity of 2.4 (Fig. 10). These sites were more stable to annealing than in undoped alumina, because they disappeared only after heating the sample at 400°C . The Brønsted acid sites generated the band at 1540 cm^{-1} with a relative intensity of 0.79.

The bending band at 1632 cm^{-1} (Fig. 10) was produced by water OH groups. This band diminished with temperature and disappeared at 500°C .

For the La doping concentration of 5 wt% the number of Lewis acid sites increased whereas the Brønsted sites disappeared (Fig. 11). Therefore, the band at 1540 cm^{-1} was not observed anymore. Since the number of Lewis acid sites increased, the band at 1442 cm^{-1} had a relative intensity of 4.12.

Cerium-doped alumina samples had variable Lewis and Brønsted acid site concentrations. In the samples with 2 wt% Ce, the number of acid sites increased in the main, being thermally stable even at 500°C (Fig. 12). At 1448 cm^{-1} these samples had an adsorption band characteristic of Lewis acid sites; it had a relative intensity of 6.71 when it was fresh and a relative intensity of 0.59 after it was heated at 500°C . Brønsted acid sites generated the band at 1540 cm^{-1} , with a relative intensity of 1.06. This intensity corresponded to 30% more Brønsted sites than in the samples doped with 2 wt% lanthanum. For Ce doping, Brønsted sites were thermoresistant even at 300°C , where the relative intensity of the corresponding band is 0.13 (Fig. 12). The band of Lewis acidity, observed at 1490 cm^{-1} , had a relative intensity of 2.07; it was also higher than in the 2 wt% lanthanum sample.

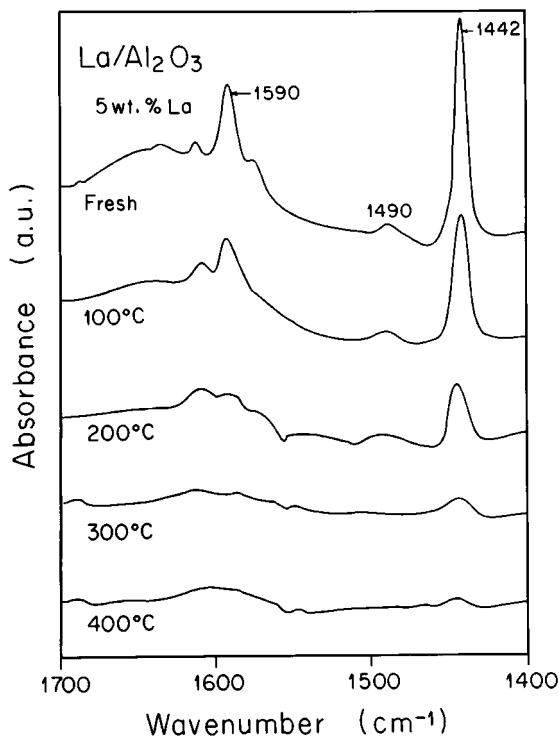


FIG. 11. FTIR spectra of pyridine adsorbed in a sol-gel $\text{La}/\text{Al}_2\text{O}_3$ sample with 5 wt% La.

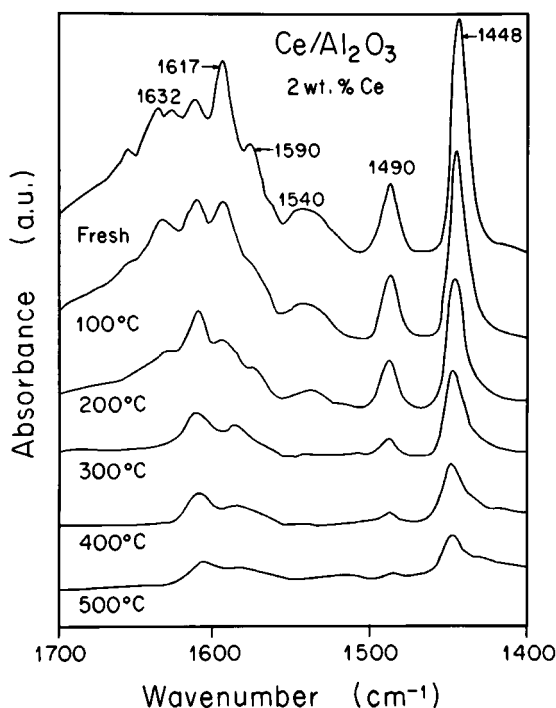


FIG. 12. FTIR spectra of pyridine adsorbed in a sol-gel $\text{Ce}/\text{Al}_2\text{O}_3$ sample with 2 wt% Ce.

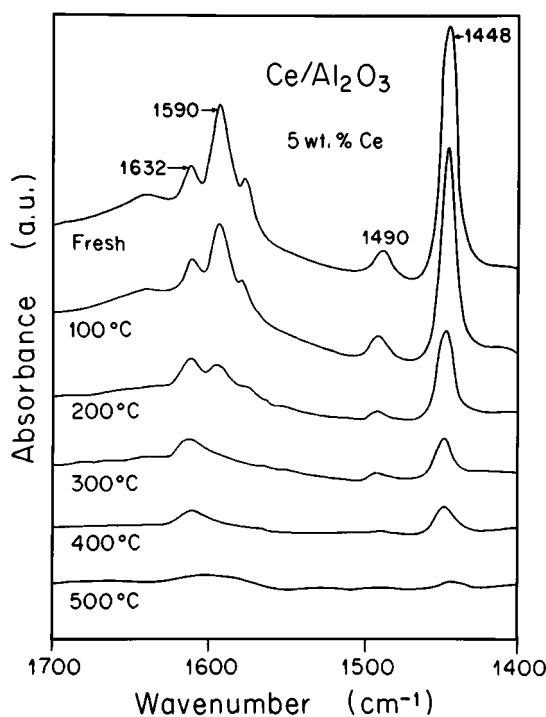


FIG. 13. FTIR spectra of pyridine adsorbed in a sol-gel $\text{La}/\text{Al}_2\text{O}_3$ sample with 5 wt% Ce.

At this Ce doping concentration, the bending vibration of OH ions of residual water and solvent in the gel gave rise to a band at 1632 cm^{-1} with an intensity decreasing with temperature (Fig. 12) because of sample dehydration.

When cerium concentration was increased to 5 wt% (Fig. 13) the Brønsted sites disappeared. The number of Lewis acid sites increased, producing an increase in the intensity of the bands at 1590 and 1448 cm^{-1} , reaching a relative intensity of 7.97. These were the samples with the highest concentration of Lewis acid sites.

4. CONCLUSIONS

When alumina was doped with La or Ce atoms and was prepared by the sol-gel technique, the doping atoms were incorporated into the alumina structure and generated structures with aluminum ions in tetrahedral symmetry. This produced an alumina-dopant interaction that stabilized alumina structures, shifting their transformations to higher temperatures. The interaction was stronger for La doping.

CeO_2 was segregated when the samples doped with Ce were heated at high temperatures, instead of forming any Ce-Al-O compound. For La doping, we observed, even after heating the sample at 1200°C , neither segregation nor the formation of LaAlO_3 phase supposed to be responsible for alumina stabilization.

Low Ce doping concentrations produced Brønsted acid sites, but they disappeared at the high doping concentrations. The number of Lewis acid sites significantly increased when the samples were doped with the high concentrations of La and Ce. These sites were more stable than in undoped alumina.

ACKNOWLEDGMENTS

We thank CONACyT (Mexico), CNRS (France), and the National Science Foundation (United States) for financial support.

REFERENCES

1. L. D. Pfefferle and W. C. Pfefferle, *Catal. Rev. Sci. Eng.* **29**, 219 (1987).
2. J. B. Peri, *J. Phys. Chem.* **69**, 220 (1965).
3. H. Knozinger and P. Ratnasamy, *Catal. Rev. Sci. Eng.* **17**, 31 (1978).
4. C. R. Narayanan, S. Srinivasan, A. K. Datye, R. Gorte, and A. Biaglow, *J. Catal.* **138**, 659 (1992).
5. B. C. Lippens and J. H. De Boer, *Acta Crystallogr.* **17**, 1312 (1964).
6. S. J. Wilson, *J. Solid State Chem.* **30**, 247 (1979).
7. Y. Mizushima and M. Hori, *J. Non-Cryst. Solids* **167**, 1 (1994).
8. G. G. Gardes, G. M. Pajonk, and S. J. Teichner, *Bull. Soc. Chim. Fr.*, 1321 (1976).
9. Y. Mizushima and M. Hori, *J. Appl. Catal.* **88**, 137 (1992).
10. A. C. Pierre and D. R. Uhlman, *J. Non-Cryst. Solids* **82**, 271 (1986).
11. A. M. Jones, Ph.D. thesis, Texas Christian University, 1974.
12. B. Imelik, M. V. Mathieu, M. Prete, and S. J. Teichner, *J. Chim. Phys. Fr.* **51**, 651 (1954).

13. G. M. Panjonk, M. B. Taghavi, and S. J. Teichner, *Bull. Soc. Chim. Fr.*, **983** (1975).
14. B. E. Yoldas, *Am. Ceram. Soc. Bull.* **54**, 286 (1985).
15. B. E. Yoldas, *J. Appl. Chem. Biotechnol.* **23**, 803 (1973).
16. B. E. Yoldas, *J. Am. Ceram. Soc.* **65**, 382 (1982).
17. B. E. Yoldas, *Mater. Sci.* **10**, 1856 (1975).
18. B. E. Yoldas, *J. Mater. Sci.* **63**, 145 (1984).
19. B. E. Yoldas, *Am. Ceram. Soc. Bull.* **54**, 289 (1985).
20. T. López, J. Méndez, R. Gómez, and A. Campero, *LatinAm. Appl. Res.* **20**, 167 (1990).
21. F. Oudet, P. Courtine, and A. Vejux, *J. Catal.* **114**, 112 (1988).
22. B. Béguin, E. Garbowski, and M. Primet, *Appl. Catal.* **75**, 119 (1991).
23. H. Schaper, E. B. M. Doesburg, and L. L. Van Reijen, *Appl. Catal.* **7**, 211 (1983).
24. H. Schaper, D. J. Amesz, E. B. M. Doesburg, and L. L. Van Reijen, *Appl. Catal.* **9**, 129 (1984).
25. M. Pijolat, M. Dauzat, and M. Soustelle, *Thermochim. Acta* **122**, 71 (1987).
26. B. Béguin, E. Garbowski, and M. Primet, *J. Catal.* **127**, 595 (1991).
27. C. Li, K. Domen, K. Maruya, and T. Onishi, *J. Catal.* **123**, 436 (1990).
28. D. D. Beck, T. W. Capeheart, and R. W. Hoffman, *Chem. Phys. Lett.* **159**, 207 (1989).
29. K. R. Krause, P. Schabes-Retchkiman, and L. D. Schmidt, *J. Catal.* **134**, 204 (1992).
30. F. Dacheille and P. Gigl, *High Temp. High Pressures* **15**, 567 (1983).
31. D. Müller, W. Gessner, H.-J. Behrens, and G. Scheller, *Chem. Phys. Lett.* **79**, 59 (1990).
32. Y. S. Kim, *Acta Crystallogr. B* **24**, 295 (1968).
33. F. R. Chen, J. G. Davis, and J. J. Fripiat, *J. Catal.* **133**, 263 (1992).
34. S. Rajagopal, T. L. Grim, D. J. Collins, and R. Miranda, *J. Catal.* **137**, 453 (1992).